

Feeding of plankton in turbulent oceans and lakes

Hans L. Pécseli¹,^{*} Jan K. Trulsen,² Jan Erik Stiansen,³ Svein Sundby,³ Petter Fossum³

¹Department of Physics, University of Oslo, Oslo, Norway

²Institute of Theoretical Astrophysics, University of Oslo, Oslo, Norway

³Institute of Marine Research, Bergen, Norway

Abstract

Analytical models for the statistical distribution of the gut content of fish larvae in a turbulent ocean environment are compared to data obtained in a field experiment. The proposed model allows the nutrition state and thereby the survival probability of plankton populations to be estimated for given conditions and parameters characterizing their environment, i.e., prey concentrations and turbulence levels. These parameters are all available in the field data. Other parameters such as the capture range and fields of view together with a characteristic time for digesting prey are assumed to be known. The analysis allows an estimate for the probability density of the gut content of plankton in terms of the number of nauplii in the gut. In particular, the analytical results give a basis for evaluating the average gut content of a given plankton population on the basis of basic information concerning the prey concentration and the turbulence intensity. Also analytical models for the prey capture rates are compared with results based on the field data. The analysis emphasizes the effects of turbulence.

Turbulence represents the most effective mixing agency met in nature on small as well as large scales. It has been anticipated (Rothschild and Osborn 1988; Osborn 1996) that turbulent motions in the surrounding flows can be important also for the encounter rate of aquatic microorganisms and their prey by bringing predators and prey close from time to time, and thereby enhance the probability of capture even without relying on self-induced motions. Thus, also the feeding processes of plankton will be influenced by turbulence. A number of observations support these ideas (Sundby and Fossum 1990; Saiz and Alcaraz 1991, 1992*a,b*; Sundby et al. 1994). For ambush predators like *Gadus morhua* L., the turbulent mixing in the surroundings will dominate the encounter rate between predators and prey. Later also the effect of self-induced locomotion has been included, considering in particular different motion patterns such as cruising and pause-travel search behavior (MacKenzie and Kiørboe 1995; Pécseli et al. 2010; Almeda et al. 2018).

Models for predator prey encounter rates form the basis of many biological applications, including the feeding rates of larval fish and the implications of environmental effects on their growth and survival (Hinrichsen et al. 2002; Lough et al. 2005). Many elements of the various models have been

tested under controlled laboratory conditions (Hill et al. 1992; Mann et al. 2005) or by numerical simulations (Lewis and Pedley 2000; Pécseli and Trulsen 2007; Pécseli et al. 2010).

The capture probability given encounter, depends on the escape strategy of the prey and conditions in the surroundings, turbulent motions in particular. Enhanced turbulence can thus have an adverse effect by reducing the capture probability of prey (MacKenzie et al. 1994). As far as the escape is concerned, we assume that it is statistically independent of other conditions, and assign it a probability $(1-P_c)$ that is assumed known, as determined for instance by laboratory investigations. The implication is that given encounter a predator will capture passively moving prey with certainty if the conditions in the flow are completely calm.

In this study, we suggest a general analytical model containing measurable parameters. These can be used to quantify the species in question and also the surrounding environment, including the turbulence conditions as determined by the specific energy dissipation rate, ϵ . Given this information, the model can predict probability densities for the gut content of, e.g., fish larvae, the average gut content in particular. We consider this to be key information for predicting the survival probability of plankton.

Methods

This study summarizes data from a field experiment and compares them with analytical results and models.

*Correspondence: hans.pecseli@fys.uio.no

This is an open access article under the terms of the Creative Commons Attribution License, which permits use, distribution and reproduction in any medium, provided the original work is properly cited.

Field experiment

Our data are obtained at Lofoten, Norway during April–May 1995 (Gytre et al. 1996). During this campaign, data were collected at five sites, see Figs. 1–2. At one of the sites (Site III), we have two data sets with different turbulence conditions.

The observational design for study of fish larvae as predators and their naupliar prey in the pelagic layer in this article is the same as the one described elsewhere (Sundby and Fossum 1990; Sundby et al. 1994) (see positions A, B, C, and D in Fig. 2). However, the representations of the turbulence in the pelagic layer were different. Previous studies (Sundby and Fossum 1990; Sundby et al. 1994) used a proxy for the ambient average turbulent energy dissipation rate ϵ obtained both by an 8-h averaged cubed wind speed (Oakey and Elliott 1982; MacKenzie and Leggett 1993) taken prior to the plankton observations from the ship (E in Fig. 2) and by data from nearby land-based weather stations divided by static stability through the mixed layer observed by a CTD (D in Fig. 2). In this study, the ambient turbulent conditions for the predators and the prey were represented by calculating the turbulent kinetic energy dissipation rate. Three different high-resolution acoustic current meters (an Ocean ADV from NORTEK, a MINILAB and an UCM from SimTronix) were mounted on a submarine tower 6.5 m above the seabed, see F in Fig. 2 (Gytre et al. 1996). All instruments were facing upward in order to minimize possible effects of the construction on the observations. All data in the present work are obtained by the UCM, which measures the three velocity components of the fluctuating flow with a minimum resolvable wavelength of approximately 6 cm.

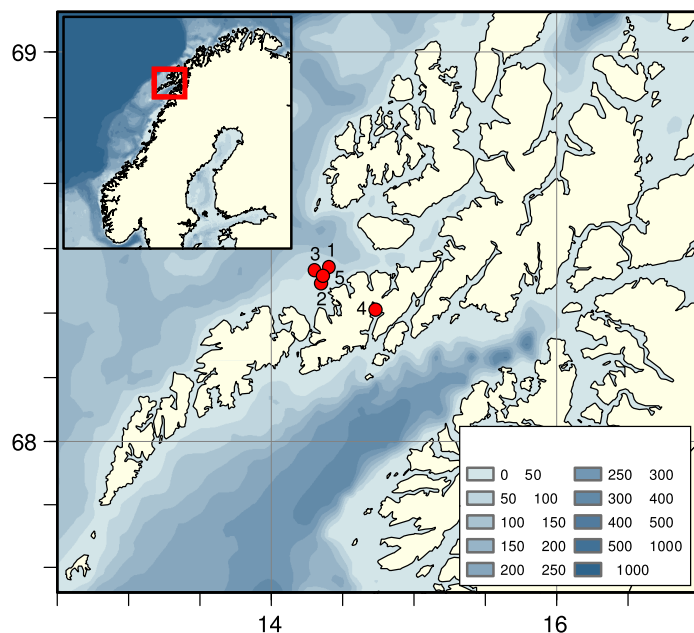


Fig. 1. Positions of the five stations near the Lofoten islands where samples were collected. The turbulence conditions at Site III had two distinct values, giving two separate data sets.

The vertical concentration profile of fish larvae was observed by a fish larvae pump (A in Fig. 2) with a capacity of approximately $0.5\text{--}0.7\text{ m}^3\text{ s}^{-1}$. A plankton net of $375\text{ }\mu\text{m}$ mesh size was attached to the fish larvae pump, and samples were made at discrete depths from 5 m to 40 m. Fish larvae were also sampled by a vertically hauled plankton net (B in Fig. 2). The opening of the net was 0.5 m^2 with a $375\text{ }\mu\text{m}$ mesh size, hauled vertically from 50 m depth, alternatively from approximately 2 m above the seabed if the water was shallower than 50 m. Fish larvae sampled from equipment A and B (Fig. 2) were inspected for gut content by counting the number of prey carcasses in the gut of fish larvae in the start-feeding phase (stage 7 larvae; Sundby and Fossum 1990). The length distribution of cod larvae from a selected site is illustrated in Fig. 3.

The entire database consists here of 3247 entries, containing the simultaneously obtained lengths and gut contents of cod larvae supported by measurements of the local specific energy dissipation rate ϵ . The data obtained by the pump (see Fig. 2) are depth-resolved, with corresponding local prey concentrations. The subset collected by the net is an average over all depths and this part of the database contains 866 entries. Since the cod larvae are migrating vertically with velocities $0.1\text{--}0.3\text{ mm s}^{-1}$ (Mauchline 1998), we do not expect any significant differences between the two data sets. Also the lengths of the nauplii in the guts were measured for a small subset consisting of 299 samples, evenly distributed over depth.

Prey data

The vertical concentration profile of naupliar prey (C in Fig. 2) was measured by a plankton pump where the seawater was pumped onto the deck of the research vessel from discrete depths of 5 m intervals and filtered through a $90\text{ }\mu\text{m}$ mesh size plankton net. Hydrographic conditions were continuously profiled with a Seabird CTD (D in Fig. 2). In Fig. 4, results for the vertical prey distribution for two sites with distinctly different turbulence conditions are shown.

An independent measurement based on 299 cod larvae gave a distribution of the lengths a of the nauplii found in the guts, see Fig. 5. The reason for the missing small size nauplii can be due to the difficulties of detecting them in the microscope, or they are not captured by cod larvae. Their sizes might be too small to give a detectable signal. The result shown in Fig. 5 partially supports an exponential distribution of nauplii sizes.

Figure 6 shows a scatter diagram for the size of cod larvae and their gut content, obtained by use of the data set from Site I. We note a tendency for larger larvae to have a larger gut content, but the correlation ($R = 0.11$) is not sufficient to allow a conclusion of substance. The scatter in larvae size (see Fig. 3) is moderate due to the preselection, and a high correlation between the size of cod larvae and their gut content cannot be supported by the present database.

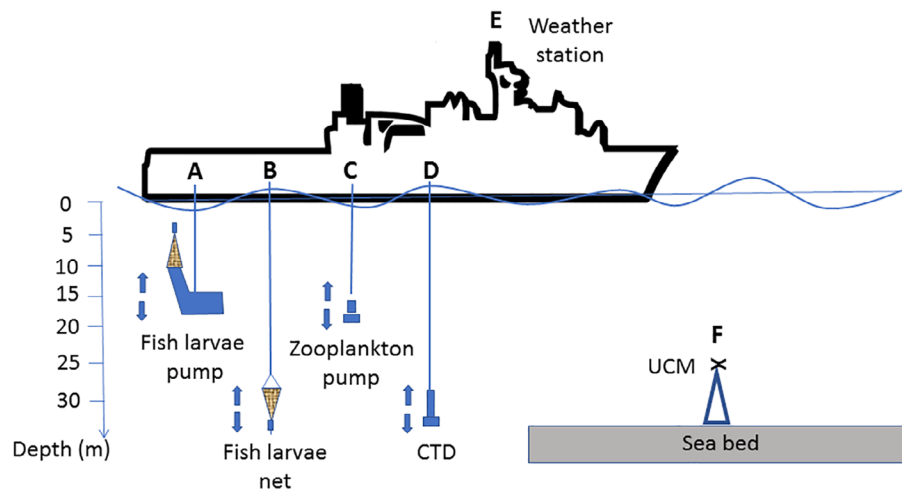


Fig. 2. Configuration of the observation procedures at stations shown in Fig. 1. Fish larvae (predators) were vertically profiled at discrete depths by the fish larvae pump (A). Analysis of gut content (number of the prey in the gut) of the fish larvae in the laboratory on board were sampled by vertically hauled fish larvae net (B). Number and size of the zooplankton prey for the fish larvae in the ambient water masses were sampled at selected depths with a zooplankton pump (C). Profiles of temperature and salinity were sampled by a seabird CTD (“conductivity, temperature, and depth”) profiler (D). Wind observations were sampled by the ship weather station (E). Turbulence measurements were made by instruments placed at the top of a 6.5 m high tower mounted on the seabed (F).

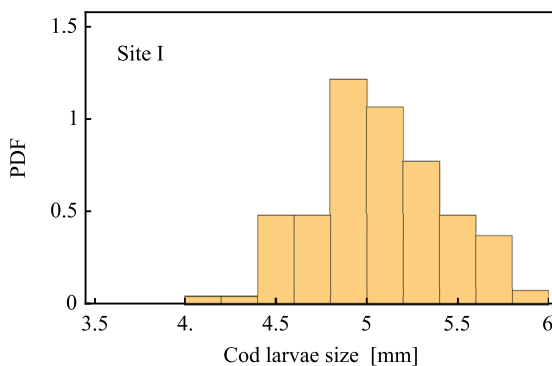


Fig. 3. Summary figure showing the length distribution of cod larvae collected at Site I by use of the fine meshed net. The figure is based on 136 entries from the database. The distribution of the lengths is moderate compared to the average value $\langle N \rangle = 5.03 \pm 0.35$ due to the selection of the larvae.

Turbulence conditions

The turbulence conditions at the present observation sites differ from the turbulent conditions of the earlier studies (Sundby and Fossum 1990; Sundby et al. 1994) in that turbulent sources other than wind mixing dominate in the present sites. Sites I, II, III, and V are all in a shallow-water region of water depths 10–25 m where turbulence is dominated by tidal mixing (Sundby et al. 1994) and swells arriving from the deep-sea region of the adjacent North Sea (Gytre et al. 1996). When the effects of tidal motions and wind are negligible, we can still have swells as a source of low-turbulence levels. The swells are temporally intermittent, but their contribution to the turbulence level is averaged over a digestion time of the fish larvae (30–60 min). This intermittency has no effect on the present data analysis.

For each set of experimental conditions, the specific average turbulence energy dissipation rate ϵ was determined by fitting experimentally obtained power spectra for velocity fluctuations and comparing them with the Kolmogorov-Obukhov power spectrum (Gytre et al. 1996). These data were obtained at a fixed installation 6.5 m above sea-bottom level. The variations in the local flow velocity are sampled with a frequency of 2 Hz, using time series of 20 min duration. The analytical Kolmogorov-Obukhov wave-number spectrum $C_K \epsilon^{2/3} k^{-5/3}$ was compared to the experimental frequency spectra by reference to the Taylor hypothesis (Wandel and Kofoed-Hansen 1962; Shkarofsky 1969; Tennekes 1975; Stiansen and Sundby 2001; Trujillo et al. 2010). The universal Kolmogorov constant is $C_K \approx 0.5 - 1.5$. By Taylor’s hypothesis, we assume $\omega \approx \beta k$, where β is a suitably defined translational velocity, here taken to be the velocity of the mean flow. A typical value for the average horizontal velocity is 5–10 cm s⁻¹, see Fig. 7. The hypothesis gives most accurate results for large velocities (Shkarofsky 1969). Implicit in the use of the hypothesis is an assumption of local homogeneity and isotropy of the small scale turbulent velocity fluctuations. The robustness of the analysis giving ϵ is tested by using slightly different values of the exponent in the power-law, e.g., ω^{-2} . Also other methods for obtaining ϵ are described in the literature (Ott and Mann 2000; Stiansen and Sundby 2001), but these usually require additional information (such as the two point structure function) that is not available for us.

Results for the experimentally obtained spectra for the three fluctuating velocity component spectra are shown in Fig. 8. Due to the closeness of sea-bottom, the vertical component has a reduced intensity at small frequencies (corresponding to long wavelengths) but the three spectra are close for high frequencies (i.e., short wavelengths), where we argue that local isotropy

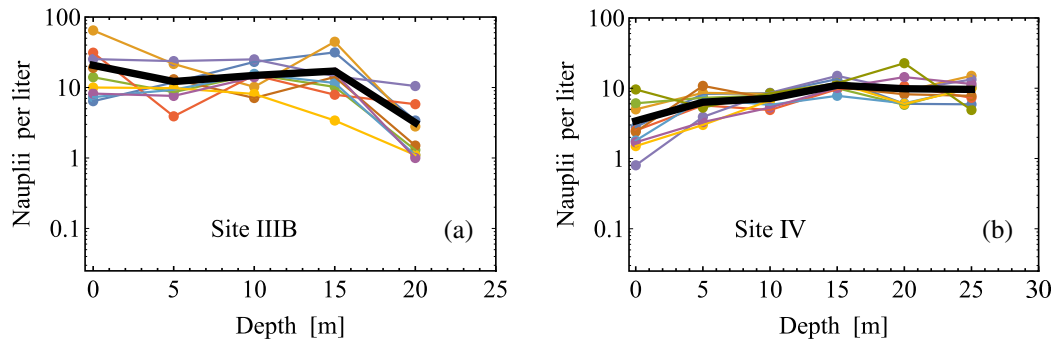


Fig. 4. Vertical distribution of prey at (a) Site IIIB—high-turbulence level, and (b) Site IV—low-turbulence level.

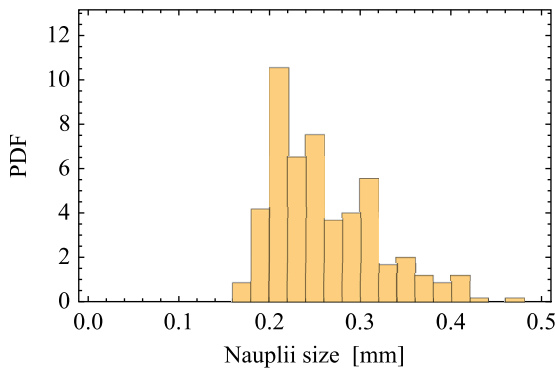


Fig. 5. Distribution of the size a of the nauplii in the guts of cod larvae. The figure is based on the gut content of 299 cod larvae distributed over all five sites.

and homogeneity has been reached. The observation that a frequency spectrum with the Kolmogorov-Obukhov exponent at high frequencies, i.e., $\omega^{-5/3}$, is a good approximation can be taken as a support for the applicability of Taylor’s hypothesis. Table 1 contains a summary of the average values of ϵ obtained for each site. The experimentally obtained spectral index agrees

with the analytical $-5/3$ -law, so the main uncertainty in the estimate of ϵ is found in the use of Taylor’s hypothesis and the uncertainty of the translational velocity being used. The experimentally obtained values of ϵ vary over the time series as can be seen in the relative variation $(\epsilon - \langle\epsilon\rangle)/\langle\epsilon\rangle$ at Site I, see Fig. 9. The figure is representative also for the other sites.

Figure 4 gives an indication of the effects of turbulence. At site IV, where the turbulence level is small, there is reduced scatter in the data, i.e., each time the vertical nauplii distribution is measured the results are similar. The same measurements carried out at a site with enhanced turbulence (such as site IIIB), gives a noticeably enhanced scatter in the results. The observation is consistent with a stronger mixing by increased turbulence levels. A similar analysis of data from the other sites supports this interpretation, although the database is not sufficiently large to give a reliable presentation of the data scatter vs. turbulence level.

Summary of analytical results

We suggest that the average content of prey in their gut provides a useful measure of the nutrition state of a plankton

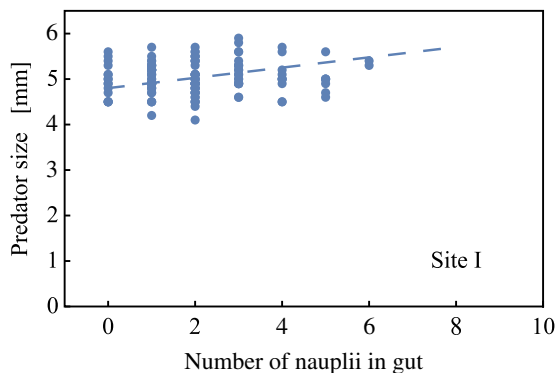


Fig. 6. Scatter diagram obtained by the data used in Fig. 3 together with the corresponding nauplii content in the guts. The dashed line is the best linear fit with correlation $R = 0.11$. The projection of the data on the vertical axis will give a result as shown in Fig. 3.

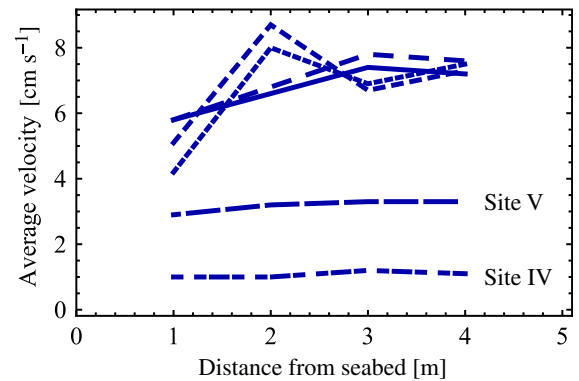


Fig. 7. The average velocities are measured at the tower, see Fig. 2, at four levels above bottom. The velocities used when applying Taylor’s hypothesis for estimating ϵ are found by the average of these at each site. Full line gives data from Site I, long dashes for Site II, and shorter dashes for Sites IIIA and IIIB. The smallest value of ϵ is found at Site IV where also the average velocity is smallest.

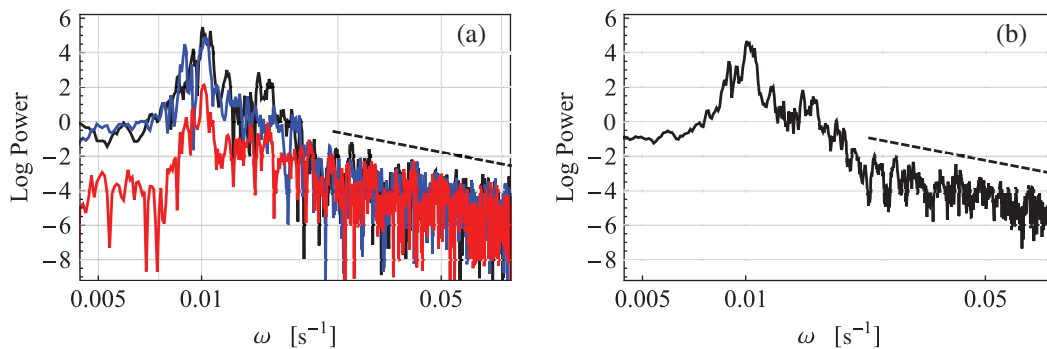


Fig. 8. Power spectra for the three velocity components as measured by the UCM at F in Fig. 2 are shown in (a), with horizontal components in blue and black, vertical in red. In (b), we show their average. Dashed reference lines have a slope of $-5/3$ as appropriate for the Kolmogorov-Obukhov spectrum.

Table 1. Summary table of field data and some quantities derived from them.

Station	$\langle L_e \rangle$ (mm)	$\langle N_T \rangle$	$\langle N_H \rangle$	n_0 (L $^{-1}$)	$\langle a \rangle$ (μ m)	ϵ (m 2 s $^{-3}$)	η_0 (mm)	τ_K (s)
I	4.685	1.89	1.99	11.22	299	1.12×10^{-6}	17.11	1.16
II	4.800	1.28	1.45	9.17	299	3.62×10^{-6}	12.77	0.64
III-A	4.723	1.86	2.09	19.74	245	5.44×10^{-5}	6.49	0.17
III-B	4.700	1.45	1.62	13.59	306	1.70×10^{-5}	8.68	0.30
IV	4.221	3.43	3.34	7.90	214	4.25×10^{-8}	38.80	5.94
V	4.689	1.39	1.26	3.25	263	2.46×10^{-6}	14.06	0.78

community. For this purpose, we need analytical expressions for the probability density on the gut content.

Analytical models for plankton guts with finite capacity

Assume that prey, nauplii for instance, are captured by planktonic predators at an average rate of μ s $^{-1}$. This quantity, to be discussed later, will depend on the parameters of the surroundings, turbulence level, prey concentration, and so on. Upon capture, prey will be digested. As a universally accepted exponential model, we assume that the digestion rate (or clearance rate) can be described by a time constant τ_d so that captured prey is consumed as $\exp(-t/\tau_d)$ with time t after capture. The time varying mass content $G(t)$ of a gut can then be modeled by the expression

$$G(t) = \sum_{j=1}^K g_j \mathcal{H}(t-t_j) \exp(-(t-t_j)/\tau_d), \quad (1)$$

representing accumulated prey in the predator's gut. Heaviside's unit step function is given as $\mathcal{H}(t)$. We introduced $g_j > 0$ as a measure for the mass of the prey labeled j , and t_j indicates its time of arrival to the gut, i.e., the capture time. Sometimes samples of prey are "overlapping" in the sense that one is captured before one or more of the previously captured samples have been digested completely. The time series of Eq. 1 will represent the time variation of the net prey mass in the predator's gut, and demonstrates in particular how the time constant τ_d is interpreted.

Field data on digestion times are sparse, but studies of for instance *Mnemiopsis leidyi* indicate that the observed values for τ_d have a large scatter and depend on the prey and the conditions in the surroundings (Granhag et al. 2011). In this study, we simplify the model by assuming τ_d to be a fixed and deterministic constant. Assuming a typical time scale for digestion to be in the range $\tau_d \sim 30 - 60$ min (Tilseth and Ellertsen 1984), it will quite often happen that prey is captured while some of those previously captured are only partially digested.

The analysis of the statistical distribution of the predator gut content can be formulated in slightly different ways. The simplest analysis addresses the number of prey in the gut. This approach is directly relevant for the comparison with our data. Another, more advanced analysis, considers the mass of prey in the gut of cod larvae as given by Eq. 1. This model can be

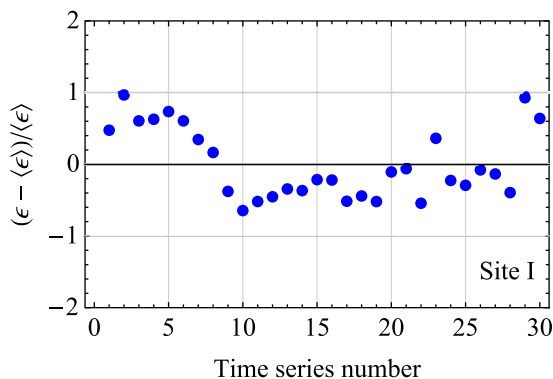


Fig. 9. The relative variation of ϵ over the different time-series obtained at Site I.

analyzed as well with a physically acceptable model (Garcia 2012) for the probability density of g . This problem is not discussed further here, but the results agree well with the following simpler analysis.

We propose a simple model for a time series that simulates the number of captured and subsequently digested prey. The series has the analytical form

$$C(t) = \sum_{j=1}^K \mathcal{H}(t-t_j) - \mathcal{H}(t-t_j-\tau_d), \quad (2)$$

The function $C(t)$ takes integer values N , depending on the number of prey in the gut at time t . The time t_d is the time needed for digestion of prey assuming that it is no longer discernible in the gut at a time $t > \tau_d$ after capture. The discrete probability density associated with the time series of Eq. 2 is known (Pécseli 2016) as

$$P_d(N) = \sum_{j=0}^{\infty} \delta_{j,N} \frac{(\mu\tau_d)^j}{j!} \exp(-\mu\tau_d), \quad (3)$$

introducing the Kronecker $\delta_{j,N}$ which is unity if $j = N$, and zero otherwise. It is interesting to note the μ and τ_d appear here only as a product and not individually. From simple dimensional arguments (Buckingham 1914), this could have been seen from the outset. The finite gut capacity can be taken into account by truncating N at some maximum integer number N_m and then normalizing the resulting distribution.

In the limit of a low number of prey captured by time unit, the probability of finding a full gut will be negligible. For that case, we can use Eq. 3 without a maximum limit for N , and find the simple expression for the average number of prey in the gut as $\langle N \rangle = \mu\tau_d$ and $\langle N^2 \rangle = \mu\tau_d + (\mu\tau_d)^2$ giving the standard deviation $\sqrt{\langle N^2 \rangle - \langle N \rangle^2} = \sqrt{\mu\tau_d}$. A set of observations will provide an estimate for $\langle N \rangle$ that can be used for estimating either the average number of prey captured per time unit, or the digestion time τ_d , when the other quantity is known.

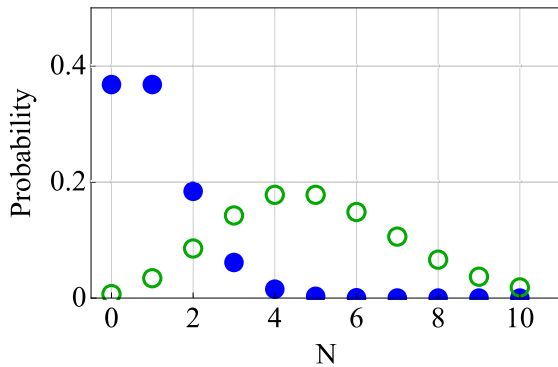


Fig. 10. Illustrations of the discrete probability density $P_d(N)$ obtained from Eq. 3, using $N_m = 10$ for $\mu\tau_d = 1$ (filled blue symbols) and 5 (open green symbols).

The finite gut capacity can be accounted for by the normalized probability density

$$P_d(N|N_m) = \frac{\exp(-\mu\tau_d)\Gamma(2+N_m)}{(1+N_m)\Gamma(1+N_m,\mu\tau_d)} \sum_{j=0}^{N_m} \delta_{j,N} \frac{(\mu\tau_d)^j}{j!}, \quad (4)$$

in terms of the $\Gamma(y)$ -function and the incomplete $\Gamma(y; z)$ -function (Abramowitz and Stegun 1972). We assume N_m to be given. The result has then no free adjustable parameters since $\mu\tau_d$ is a measurable quantity. Representative results are shown in Fig. 10 for two values of $\mu\tau_d$. Also in this case, we can determine averages and mean square averages, but the analytical expressions become lengthy. Illustrative results are shown in Fig. 11. The standard deviation is small when most guts are either empty, $N \gtrsim 0$, or full, $N \lesssim N_m$.

Error estimate of the maximum number of nauplii in the gut

If the number of prey in the gut is large, some will be small, some large, and the actual net gut content would be close to the one obtained by assigning all prey the same size, i.e. the average size. The question is how large the number M of prey in the gut has to be for this argument to apply?

A model problem will be considered here. Assume that prey has a probability density $Q(a) = \exp(-a/\langle a \rangle)/\langle a \rangle$ for size a . This is a “worst case” scenario by over-representing very small nauplii in the guts. We determine the conditional probability density $P_M(b)$ associated with the size parameter $b = \sum_{i=1}^M a_i \geq 0$ with all a_i following the same exponential probability density $Q(a)$. The assumed probability density $Q(a)$ is in agreement with observations at least for large a , see Fig. 5. Assuming M to be the number of prey present in the gut at the same time, it can be demonstrated that

$$P_M(b) = \frac{b^{M-1}}{\langle a \rangle^M \Gamma(M)} \exp\left(-\frac{b}{\langle a \rangle}\right). \quad (5)$$

For given $M > 1$, the relative error in assigning b the value $M\langle a \rangle$ can be found by taking the average value $\sigma_M \equiv \sqrt{\langle (b - M\langle a \rangle)^2 \rangle} / (M\langle a \rangle)$ obtained by Eq. 5. The result for the relative error is simply $\sigma_M = 1/\sqrt{M}$. For $M \geq 10$ (corresponding to the assumed value of N_m), we can assume the size parameter b to be given as $M\langle a \rangle$ with an accuracy better than 30%. We thus find that the relative error is significantly reduced already at $M \sim 10$ so that our assumptions in the modeling are justified.

Prey flux estimates

The foregoing results assume that the parameters μ and τ_d are known. Concerning τ_d , the digestion time, we expect it to be specific for the species and their age, and to depend also on the

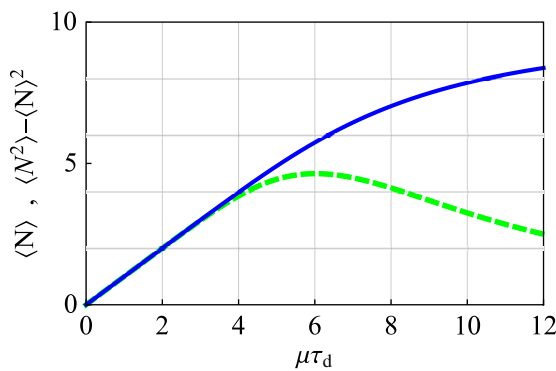


Fig. 11. The variation of the average $\langle N \rangle$ with solid line, and $\langle N^2 \rangle - \langle N \rangle^2$ with dashed line, as functions of $\mu\tau_d$ as obtained by use of Eq. 4 with $N_m = 10$.

temperature and other parameters of the surroundings. The values $\tau_d \sim 30 - 60$ min quoted before are representative for the ambient temperature in the present data set. The prey flux into the gut μ is representing a more complex process. We find it to be an advantage to separate μ into an encounter rate, or clearance rate, J_e and a capture probability P_c , give the encounter. Assuming the two to be independent, we have $\mu = J_e P_c$. Previous studies (Rothschild and Osborn 1988; Osborn 1996) discussed the encounter rate for ambush predators, but included also the effects of self-induced motions. In these early studies, capture was assumed to be independent of the turbulence level. Only the inertial subrange of turbulence was considered. The importance of also the viscous subrange (relevant for the present study) was realized later (Pécseli and Trulsen 2007; Pécseli et al. 2012), see also the review by Kiørboe (2008).

The encounter rate depends on the species, their self-induced motions, the prey and its motion strategies, light conditions, and finally also motions in the surrounding waters and combinations of all these effects (Fiksen et al. 1998). We can separate the parameters contributing to J_e into species related and environment related. All these effects have been studied in the past, mostly in laboratory and by numerical simulations as summarized in the following. A brief summary of clearance rates under turbulent conditions can be found in the literature (Saiz et al. 2003). In this study, we will emphasize the consequences of the motions, turbulent variations in particular, of the water. For general conditions, both the species and environment related effects will be important, although not necessarily at the same time. Travel-pause predators (MacKenzie and Kiørboe 1995) can have intervals where the turbulent mixing is contributing most to the encounter with prey and the analysis can be separated into different time intervals accordingly as illustrated by Pécseli et al. (2010).

To model the turbulence-induced encounter rate, we distinguish motions on the inertial and the viscous subranges of the turbulence. It has been argued (Pécseli and Trulsen 2007; Pécseli et al. 2012) that the separation length is found approximately at a characteristic scale size of $\eta_0 \approx 13\eta$ in terms of the

classical Kolmogorov scale $\eta \equiv (\nu^3/\epsilon)^{1/4}$ where ν is the specific viscosity of the water (Tennekes and Lumley 1972). The separation of the viscous and inertial subranges of turbulence was illustrated by Pécseli et al. (2012) using the second-order velocity structure function. We introduce an encounter radius R_c that has to be compared to η_0 in order to distinguish the two turbulent subranges. Based on laboratory observations, the encounter range R_c , or radius of interception (Gerritsen and Strickler 1977), is defined as the distance from the fish larvae's eye to the prey when the larva changed its motion pattern to chase its prey (Sundby and Fossum 1990). The "vision distance" for a fish larvae is not the same as "reaction distance." For a typical first feeding cod larvae (5 mm long), the "reaction distance" is 0.5–1.0 body lengths measured from the mouth (Tilseth and Ellertsen 1984; Sundby and Fossum 1990). When $R_c < \eta_0$, we have the analytical relations $J_e \approx C_\nu n_0 \chi(\theta) (\epsilon/\nu)^{1/2} R_c^3$, with an empirically determined constant $C_\nu \approx 1$. Also the field of view is important for the encounter rate (Almeda et al. 2018), and is here included by the factor $\chi(\theta)$, accounting for the effects of an opening angle θ for a conical field of view. For a hemispherical field of view, we have $\chi(\pi/2) \approx 0.8$, while $\chi(\pi/4) \approx 0.45$. An empirical formula for all θ can be found (Pécseli et al. 2014) that serves for both the inertial and viscous subranges. The prey flux is directly proportional to the concentration of prey in the environment, here denoted n_0 . The encounter range (or range of interception) R_c will depend on the size and age of the predator and also of the prey being encountered (Kiørboe 2008). Here, we assume a value taken as an average of encountered prey.

Models more general than those proposed by Rothschild and Osborn (1988) or Osborn (1996) allow for the capture probability to depend on the turbulence level. If the surrounding water is in turbulent motion, there will be a finite probability for prey to be transported out of the interaction region before capture and be lost. This probability will depend on the predator species as well as prey and in particular also on the intensity of the turbulence. Large turbulence levels can thus enhance the relative motions between predator and prey to an extent where the capture is inhibited because the time available for capture is too small (Marrasé et al. 1990; MacKenzie et al. 1994; Kiørboe and Saiz 1995; Saiz and Kiørboe 1995; Pécseli et al. 2012). Due to a competition between these two effects, i.e., the enhanced encounter rate and the reduced capture probability, there will be an optimum level of turbulence for predation. This optimum will be different for different species. The prey capture rate as a function of the turbulence level will have a "dome shape," with a maximum at some intermediate turbulence level as argued by MacKenzie et al. (1994).

To give a phenomenological model for the finite capture probability (MacKenzie et al. 1994), we assume that it can be modeled by a single characteristic time t_m , assuming that prey is not captured if it spends less time in the volume of interception, while it is captured with certainty (as far as this process

is concerned) if it stays a time longer than t_m . The probability distribution $P_\tau(\tau)$ of times spent by a particle in a volume embedded in a turbulent flow has been studied both numerically (Pécseli and Trulsen 2010; Pécseli et al. 2012) and in laboratory experiments (Jørgensen et al. 2005). Also more advanced models with several time scales have been proposed. Thus, more generally, it was assumed that capture was impossible if prey spent less time than a certain minimum τ_1 within the encounter range of the predator. The capture probability then gradually increased until it became close to certain for times larger than some τ_2 . The present simplified model replaces τ_1 and τ_2 with one characteristic time $\tau_1 < t_m < \tau_2$. To the accuracy of the data to be discussed in the following, we believe that the present simpler model will suffice. The model used for the capture probability in this study is different from the one used by MacKenzie et al. (1994), although that work is also based on times available for capture.

The escape of prey by its self-induced motion is assumed to be a statistically independent process and can be included by an empirical multiplier $P_{es} \leq 1$ which has to be determined in a laboratory, for instance. Although the individual escape processes have been studied in detail (Kjørboe 2008), only little is known about the average escape probability as such for the prey and predator species relevant in the following.

For ambush predators, we can now write a compact form for the flux into the gut as

$$\mu = C_\nu n_0 R_c^3 \left(\frac{\epsilon}{\nu}\right)^{1/2} \chi(\theta) P_c \int_{t_m \sqrt{\epsilon/\nu}}^{\infty} P_\tau(\tau') d\tau', \quad (6)$$

taking R_c to be in the viscous subrange of the turbulence. The integral accounts for the variation of the capture probability with the parameters of the problem. In Eq. 6, we recognize two length scales, the range of interception R_c and the average prey separation $n_0^{-1/3}$, with the product $n_0 R_c^3$ entering as a dimensionless parameter for the problem. We have μ being linearly proportional to the prey concentration n_0 . The probability of two prey simultaneously entering the range of interception is assumed negligible. This implies that a predator can concentrate on one sample of prey at a time. Analytical approximations and tables of the probability density $P_\tau(\tau)$ needed in Eq. 6 can be found in the literature for various forms of the encounter and capture volumes (Pécseli et al. 2012). These results are given in terms of a normalized time $t_m \sqrt{\epsilon/\nu}$. Given the input parameters n_0 and ϵ , we are thus in a position to give estimates for the average gut content of fish larvae by use of Eq. 4 when the organisms are characterized by their capture range R_c and opening angle θ for their field of view. An even more ambitious result is an estimate for the entire probability density of prey in the gut.

It has been suggested (Pécseli et al. 2012; Pécseli and Trulsen 2016) that enhanced turbulence levels can be seen as “noise” that will make it difficult for a predator to discriminate

signals from prey by disturbing the hydro-mechanical signals detected by the predators (Kjørboe and Visser 1999). This effect will contribute to make the “dome shape” more pronounced by reducing the capture rate for large ϵ . As a “rule of thumb” we argue that if $10\tau_K \leq t_m$, we can expect that the turbulence-induced noise-signal experienced by a predator will be disturbing and partially masking the flow disturbance induced by moving prey. For Site IIIB, we expect this to be the case marginally, but for the other stations this effect will have minor consequences and it is thus not included in the analysis.

Results

Many of the experimental data and observations are of interest themselves. We give particular attention to data that can be compared to analytical predictions. These are the distribution $P_d(N)$ of the gut content, and the rate μ of captured prey.

Comparison of analytical results and field data

The results from the analytical model are compared with data obtained at Lofoten in which samples of predators (i.e., cod larvae) were collected by two different methods: (1) a fine meshed net moved slowly from the seabed to the surface and (2) a pump (“HUFSA”) placed at selected positions 5 m, 10 m, 15 m, 20 m, 25 m, and 30 m below the surface. The pump may in principle cause some damage to the collected fish larvae. The quality of these data has to be verified by the other collection methods which do not have this damaging effect. On the other hand, the depth information is lost in this latter case.

In Table 1, we present a summary of averaged data as they are used for the comparison with analytical results. The set of observations at a given site will be considered as realizations belonging to an ensemble with the given macroscopic parameters. The average number $\langle N_H \rangle$ of nauplii in gut is obtained by the reduced database found by using a fine meshed net moved slowly from the sea-bottom to the surface, while $\langle N_T \rangle$ refers to the full data set. The cod larvae mean length is $\langle L_\ell \rangle$, the concentration of nauplii in the surroundings is n_0 , and the mean length of nauplii is $\langle a \rangle$. The specific turbulent energy dissipation is ϵ , and the derived effective Kolmogorov length η_0 . We used $\nu = 1.5 \text{ mm}^2 \text{ s}^{-1}$ for the kinematic viscosity of saline seawater (Sharqawy et al. 2010, 2012). The last column gives the Kolmogorov time scale $\tau_K \equiv \sqrt{\nu/\epsilon}$.

The encounter radius R_c is an important parameter for the analysis (Gerritsen and Strickler 1977). In detail, it varies with species, and will in general depend on parameters in the surroundings (Fiksen et al. 1998), such as light conditions for visual predators. We argue here that the range of interception R_c (or encounter radius) can be taken to be in proportion to the size L_ℓ of the fish larvae. The information of the size of the larvae is then used for determining whether the relevant

length scale fall in the viscous or in the inertial range of the turbulence. If we assume (Tilseth and Ellertsen 1984) a capture range $R_c \approx (0.5 - 1.0)L_v$, we find from Table 1 the viscous subrange to be the most relevant one for all cases here.

Probability density for the gut content

The largest number of nauplii in a gut was found to be 12, and this number was observed only once, while 11 and 10 were both seen four times, while 9 nauplii are found more frequently. In the following, we use $N_m = 10$ for all fish larvae. The estimated distributions of the gut contents are shown in Fig. 12, based on data obtained by the fine meshed net (see Fig. 2). The net gives the least damage to the cod larvae, and these data are therefore analyzed separately. Filled circles in Fig. 12 give results derived by the analytical model in Eq. 3 by adjusting the parameter $\mu\tau_d$ so that the average corresponds to the observed value of $\langle N \rangle$. The analysis was repeated with $N_m = 9$, giving modifications that were noticeable only for Site IV. In order to quantify the difference between the model results and the observations, we note that for small $\mu\tau_d$, the model predicts $(\langle N^2 \rangle - \langle N \rangle^2) / \langle N \rangle = 1$. The same quantity is 1.18 when taken as an average for all the data sets shown in Fig. 12. We find this agreement sufficiently convincing to allow the model being used more generally. For completeness, we included with a thin dashed line in Fig. 12 also the results using all data.

The turbulence level is high for Site IIIA, see Table 1. Enhanced turbulence has an adverse effect on the capture rate, but the prey concentration for Site IIIA is on the other hand high, so that the guts have a relatively high content nonetheless. The analytical model is accounting for this. Fitting the

model in Eq. 3 to the data, we can estimate the parameter $\mu\tau_d$. Assuming τ_d known, we can then find the amount μ of captured prey per second. The results found this way will contain contributions from the prey concentration, the encounter rate, and the capture probability.

We believe the basic form for the probability density given by Eq. 3 to be universal. Details like predation strategy, and so forth, enter through the capture rate μ .

Average prey capture rate estimates

To compare the field data with the analytical model, there are several possibilities. We illustrate the consequences of the “dome shaped” capture probability (MacKenzie et al. 1994; Jenkinson 1995). In Fig. 13, the analytical result is shown (in a double logarithmic presentation) in terms of the normalized quantity $\mu t_m (R_c^3 n_0)^{-1}$ as a function of the normalized variable $t_m (\epsilon/\nu)^{1/2}$. This is relevant for the viscous subrange of turbulence. We use t_m as a time parameter characterizing the capture probability. The decrease in capture probability originating from the escape reactions of the nauplii is assumed to be incorporated in t_m . The “dome shape” can be noted in the analytical results, indicating an optimum level of turbulence for the predator. The results for the average gut content, found by use of the fine meshed net at the five stations, are inserted by large filled blue circles. Smaller filled red circles give results obtained by use of all available data, i.e., also those obtained by pumps at selected depths. To illustrate the sensitivity of the model to the assumed shape of the encounter volume, we show in Fig. 13 results for both hemispherical, $\theta = \pi/2$, and conical, $\theta = \pi/4$, capture volumes. For small ϵ , the results for the conical case are below those for the hemisphere due to the

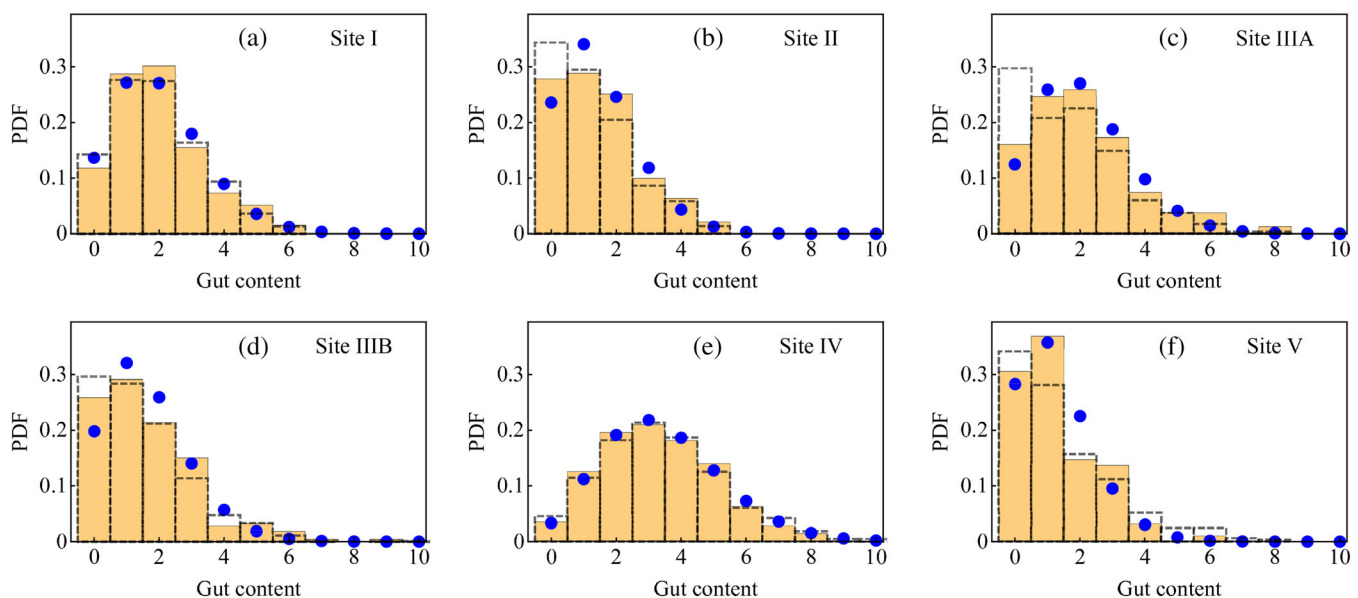


Fig. 12. Illustrations of the distributions of the number of nauplii in the gut of *Gadus morhua* L. larvae collected by a fine meshed net moved slowly from the seabed to the surface at Sites I through V (a–f). Corresponding analytical results by Eq. 3 are given by filled circles. We have $\mu\tau_d = 1.99, 1.45, 2.09, 1.62, 3.34$, and 1.26 . Thin dashed lines give the results when all data are included in the analysis.

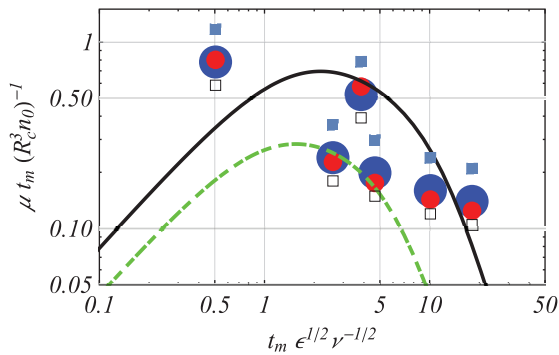


Fig. 13. Solid line gives the analytical result for the normalized prey flux $\mu t_m (R_c^3 n_0)^{-1}$ to the predator as a function of the normalized variable $t_m (\epsilon/\nu)^{1/2}$, for the viscous subrange of turbulence for a hemispherical field of view. The dashed line is the result for a cone with opening angle $\theta = \pi/4$. The data points (red and blue circles) are determined by data from the observational sites, see Fig. 1 and Table 1. The parameters used for the field data analysis are $R_c = 2L_\ell$, $t_m = 3$ s, and $\tau_d = 45$ min. Small squares (full and open symbols) correspond to $\tau_d = 30$ min and $\tau_d = 60$ min, respectively. The sites corresponding to the different symbols can be identified by the different ϵ -values. The first point thus corresponds to Site IV, with the smallest turbulence level.

smaller contact surface, i.e., smaller $\chi(\theta)$. For large ϵ , an additional reduction is found due to the reduction in capture probability, i.e., shorter prey transit times. To illustrate the sensitivity of the results to changes in the digestion time τ_d , we inserted data obtained by $\tau_d = 30$ min (■) and $\tau_d = 60$ min (□) obtained by the full data set. The ranges of acceptable digestion times (30 – 60 min) are accommodated within our results, but we find 45 min to give the best fit to the analytical curve with $\theta = \pi/2$ within a factor 2 on average for all six parameters. The conditions at Sites I and V appear to be close to the theoretical optimum where the enhancement of encounter rates, J_e , due to turbulent mixing, balances the reduction in the capture rate, P_c , which is also caused by turbulence.

Although the uncertainties cannot be ignored, we find that the field data support models for the adversary effects of enhanced turbulence, which is a basic element in the “dome shaped” capture probability discussed in the literature (MacKenzie et al. 1994). Moderate turbulence levels will be an advantage (for the predator) by enhancing the encounter rate between predators and prey, in particular for ambush predators with small self-induced motions (Rothschild and Osborn 1988; Osborn 1996). Large turbulence levels are a disadvantage by reducing the capture probability (Marrasé et al. 1990).

Discussion

Probability density of the gut content

The analytical model Eq. 3 has no free or adjustable parameters. Given the mathematical form, it depends solely on one variable, $\mu\tau_d$, which has to be chosen consistently with the data. The precise value of the maximum gut content N_m is

immaterial for populations with a small average gut content. When filled guts become frequent, N_m can be estimated by the maximum value of prey found in the guts. The uncertainty of this estimate was discussed before.

We distinguished two methods for collecting plankton, a fine meshed net and a pump, see Fig. 2. Comparing the gut contents from the two methods, see Fig. 12, we note a systematic overpopulation of empty guts (best seen for Site IIIA) when we include also data obtained by use of the pump. We take this as evidence that the pump is damaging plankton by making a significant part of them regurgitate. Data obtained by pumps like these should be interpreted with this possibility in mind.

In our study, we took the digestion time τ_d to be constant. In principle, it is possible for τ_d to depend on the gut content. Our data give no support for such models. Should that be the case, we would observe a systematic overpopulation for small or for large gut contents as compared to our model. It is possible that such a relation can be found by studies of populations where full guts are more frequent than in our database.

Encounter and capture rates

The capture rate μ , entering as a part of the argument of the probability density for the gut content, is an important parameter and it is desirable to find analytical expressions for it. The problem has been studied in the literature (Rothschild and Osborn 1988; Osborn 1996) and we gave a summary of our model before (Pécseli et al. 2014). We separated the problem into an encounter rate J_e and a capture probability P_c , so that $\mu = J_e P_c$. The capture probability was determined empirically in terms of a time t_m needed for capture, where we here used a simplified version of more general results (Pécseli et al. 2012). The time t_m has to be determined by laboratory observations. The model as such does not otherwise contain any other free parameters. The encounter rate on the other hand contains several parameters all subject to some uncertainties.

We distinguish uncertainties originating from the measurements, and those relating to the input data used in the analysis, R_c , t_m , and τ_d . The uncertainties in these latter parameters are discussed in the literature (Gerritsen and Strickler 1977; Tilsseth and Ellertsen 1984; Sundby and Fossum 1990; Granhag et al. 2011), and for applications of our results, they can be accounted for by repeating the analysis with other input parameters. We gave examples for different values of τ_d in Fig. 13.

The uncertainties in our database concern the turbulence parameter ϵ , and the data for cod larvae and their prey. The observed number N of prey in a gut is most likely an underestimate, since it is easier to overlook prey than to count one twice.

The lengths of cod larvae L_ℓ enter through the estimate for their capture range R_c . Due to the preselection of cod larvae,

this scatter is moderate with a typical distribution shown in Fig. 3.

The prey concentration n_0 is assigned one value at each site. The depth variation observed, see Fig. 4, does not justify any detailed model for the variations in n_0 . The spatio-temporal intermittency will have more practical importance, but in our case, the averaging over a digestion time makes also this variation of little consequence.

The uncertainty or scatter in the lengths of prey a is of minor importance, and enters only in justifying an element in the analytical estimates. It would be more important if full guts had been frequent.

The relative scatter of ϵ -values over the time-series entering the analysis is illustrated in Fig. 9. This relative scatter is typically less than a factor of 2. For Site IV with the smallest turbulence level, the scatter is smaller. A systematic error in the estimate for the specific turbulent energy dissipation ϵ originates from the use of Taylor's hypothesis. This error is not well understood, although the hypothesis is widely used. For strong turbulence, it is generally agreed that the hypothesis is sound (Shkarofsky 1969), but for low-turbulence levels similar studies are lacking. We use the measured mean flow to obtain a relation between frequencies and wave numbers without including a possible correction due to the velocity component of large scale eddies (Wandel and Kofoed-Hansen 1962; Tennekes 1975; Stiansen and Sundby 2001). This will give rise to a systematic underestimate of ϵ . This error will affect all data points in nearly the same way, and changes due to this effect will move the data points nearly like a "block". This error is of the same order of magnitude as the random error that can be estimated by comparing the values of ϵ obtained by the individual measurements (typically once per 20 min). Implicit in the analysis we have taken the ϵ -value at 6 m above bottom level to be representative for all depths. Referring to the discussion of Fig. 4, this seems to be acceptable. Our conditions are different from purely wind-driven turbulence, where there are empirical models for the depth variation $\epsilon \approx 5.8 \times 10^{-9} W^3/z$ with W in ms^{-1} and the depth z in m (MacKenzie and Leggett 1993). In our case, the forcing of the turbulence is at the bottom due to the velocity shear, and from the top mostly by swells.

The actual local viscosity ν of seawater was not measured. It depends for instance on salinity, which was not determined independently. We assume this uncertainty to be immaterial in comparison to other uncertainties of parameters entering the models.

Based on our analytical results in Eq. 3 and the results for the rate of captured prey μ , we can explain the trends found in Fig. 13. By choosing a set of physically and biologically acceptable parameters τ_d , R_c , and t_m , we succeeded in obtaining a fair agreement between the model and observations for the gut content probability density and for the capture rate. The value for the minimum time needed for capture, t_m , in particular appears large, but it represents an average of the

minimum time required for capture and the time needed for capture with large probability (Pécseli et al. 2012). With this in mind, we find the value $t_m = 3$ s to be reasonable. The most sensitive parameter is R_c by entering to the power 3. The analysis and the data support, in particular, elements of a "dome shaped" capture probability (MacKenzie et al. 1994) in the sense that we find a decreasing trend in the average capture probability for increasing large turbulence levels.

For the cod larvae in this study, we found that they on average capture prey in excess of the minimum of 1–3 nauplii per hour needed for survival (Sundby et al. 1994). This minimum corresponds to $\mu\tau_d \approx 0.75 - 2.25$ for a digestion rate $\tau_d \approx 45$ min. On the other hand, prey is not found to be in abundance either, except for Site IV with the smallest turbulence level. Our model allows the survival probability of plankton populations to be estimated for given conditions and parameters characterizing their environment, i.e., in terms of prey concentrations and turbulence levels. Inclusion of finite gut content is of limited importance for analyzing the present data set, but can be important for general applications of the model.

This study refers to ambush predators, *Gadus morhua* L., but given the agreement between data and analysis, we expect that our result can be more generally applied when self-induced motions of predators are also accounted for. For travel-pause predators, the extension of the analysis is relatively simple (Pécseli et al. 2010).

The present problem is interesting also by its cross disciplinary nature: it involves fluid dynamics, marine biology, and also signal analysis.

References

- Abramowitz, M., and I. A. Stegun. 1972. Handbook of mathematical functions with formulas, graphs, and mathematical tables. Dover.
- Almeda, R., H. Someren Gréve, and T. Kjørboe. 2018. Prey perception mechanism determines maximum clearance rates of planktonic copepods. *Limnol. Oceanogr.* **63**: 2695–2707. doi:10.1002/lno.10969
- Buckingham, E. 1914. On physically similar systems; illustrations of the use of dimensional equations. *Phys. Rev.* **4**: 345–376. doi:10.1103/PhysRev.4.345
- Fiksen, Ø., A. C. W. Utne, D. L. Aksnes, K. Eiane, J. V. Helvik, and S. Sundby. 1998. Modelling the influence of light, turbulence and ontogeny on ingestion rates in larval cod and herring. *Fish. Oceanogr.* **7**: 355–363. doi:10.1046/j.1365-2419.1998.00068.x
- Garcia, O. E. 2012. Stochastic modeling of intermittent scrape-off layer plasma fluctuations. *Phys. Rev. Lett.* **108**: 265001. doi:10.1103/PhysRevLett.108.265001
- Gerritsen, J., and J. R. Strickler. 1977. Encounter probabilities and community structure in zooplankton: A mathematical model. *J. Fish. Res. Board Can.* **34**: 73–82. doi:10.1139/f77-008

- Granhag, L., L. F. Möller, and L. J. Hansson. 2011. Size-specific clearance rates of the ctenophore *Mnemiopsis leidyi* based on in situ gut content analyses. *J. Plankton Res.* **33**: 1043–1052. doi:[10.1093/plankt/fbr010](https://doi.org/10.1093/plankt/fbr010)
- Gytre, T., J. E. O. Nilsen, J. E. Stiansen, and S. Sundby. 1996. Resolving small scale turbulence with acoustic Doppler and acoustic travel time difference current meters from an underwater tower, p. 442–450. *In* OCEANS '96 MTS/IEEE, Conference proceedings, Vols. 1–3/Supplementary proceedings: Coastal ocean - prospects for the 21st century. Marine Technol Soc, OES, IEEE. doi:[10.1109/OCEANS.1996.572797](https://doi.org/10.1109/OCEANS.1996.572797)
- Hill, P. S., A. R. M. Nowell, and P. A. Jumars. 1992. Encounter rate by turbulent shear of particles similar in diameter to the Kolmogorov scale. *J. Mar. Res.* **50**: 643–668. doi:[10.1357/002224092784797539](https://doi.org/10.1357/002224092784797539)
- Hinrichsen, H.-H., C. Möllmann, R. Voss, F. W. Köster, and G. Kornilovs. 2002. Biophysical modeling of larval Baltic cod (*Gadus morhua*) growth and survival. *Can. J. Fish. Aquat. Sci.* **59**: 1858–1873. doi:[10.1139/f02-149](https://doi.org/10.1139/f02-149)
- Jenkinson, I. R. 1995. A review of two recent predation-rate models: The dome-shaped relationship between feeding rate and shear rate appears universal. *ICES J. Mar. Sci.* **52**: 605. doi:[10.1016/1054-3139\(95\)80075-1](https://doi.org/10.1016/1054-3139(95)80075-1)
- Jørgensen, J. B., J. Mann, S. Ott, H. L. Pécseli, and J. K. Trulsen. 2005. Experimental studies of occupation and transit times in turbulent flows. *Phys. Fluids* **17**: 035111. doi:[10.1063/1.1863259](https://doi.org/10.1063/1.1863259)
- Kjørboe, T. 2008. A mechanistic approach to plankton ecology. Princeton Univ. Press.
- Kjørboe, T., and E. Saiz. 1995. Planktivorous feeding in calm and turbulent environments, with emphasis on copepods. *Mar. Ecol. Prog. Ser.* **122**: 135–145. doi:[10.3354/meps122135](https://doi.org/10.3354/meps122135)
- Kjørboe, T., and A. W. Visser. 1999. Predator and prey perception in copepods due to hydromechanical signals. *Mar. Ecol. Prog. Ser.* **179**: 81–95. doi:[10.3354/meps179081](https://doi.org/10.3354/meps179081)
- Lewis, D. M., and T. J. Pedley. 2000. Planktonic contact rates in homogeneous isotropic turbulence: Theoretical predictions and kinematic simulations. *J. Theor. Biol.* **205**: 377–408. doi:[10.1006/jtbi.2000.2073](https://doi.org/10.1006/jtbi.2000.2073)
- Lough, R. G., L. J. Buckley, F. E. Werner, J. A. Quinlan, and K. Pehrson Edwards. 2005. A general biophysical model of larval cod (*Gadus morhua*) growth applied to populations on Georges Bank. *Fish. Oceanogr.* **14**: 241–262. doi:[10.1111/j.1365-2419.2005.00330.x](https://doi.org/10.1111/j.1365-2419.2005.00330.x)
- MacKenzie, B. R., and W. C. Leggett. 1993. Wind-based models for estimating the dissipation rates of turbulent energy in aquatic environments: Empirical comparisons. *Mar. Ecol. Prog. Ser.* **94**: 207–216. doi:[10.3354/meps094207](https://doi.org/10.3354/meps094207)
- MacKenzie, B. R., T. J. Miller, S. Cyr, and W. C. Leggett. 1994. Evidence for a dome-shaped relationship between turbulence and larval fish ingestion rates. *Limnol. Oceanogr.* **39**: 1790–1799. doi:[10.4319/lo.1994.39.8.1790](https://doi.org/10.4319/lo.1994.39.8.1790)
- MacKenzie, B. R., and T. Kjørboe. 1995. Encounter rates and swimming behaviour of pause-travel and cruise larval fish predators in calm and turbulent laboratory environments. *Limnol. Oceanogr.* **40**: 1278–1289. doi:[10.4319/lo.1995.40.7.1278](https://doi.org/10.4319/lo.1995.40.7.1278)
- Mann, J., S. Ott, H. L. Pécseli, and J. K. Trulsen. 2005. Turbulent particle flux to a perfectly absorbing surface. *J. Fluid Mech.* **534**: 1–21. doi:[10.1017/S0022112005004672](https://doi.org/10.1017/S0022112005004672)
- Marrasé, C., J. H. Costello, T. Granata, and J. R. Strickler. 1990. Grazing in a turbulent environment: Energy dissipation, encounter rates, and efficacy of feeding currents in *Centropages hamatus*. *Proc. Natl. Acad. Sci. USA* **87**: 1653–1657. doi:[10.1073/pnas.87.5.1653](https://doi.org/10.1073/pnas.87.5.1653)
- Mauchline, J. 1998. The biology of calanoid copepods. *Adv. Mar. Biol.* **33**: 1–710. doi:[10.1016/S0065-2881\(08\)60233-3](https://doi.org/10.1016/S0065-2881(08)60233-3)
- Oakey, N. S., and J. A. Elliott. 1982. Dissipation within the surface mixed layer. *J. Phys. Oceanogr.* **12**: 171–185. doi:[10.1175/1520-0485\(1982\)012j0171:DWTSMI;2.0.CO;2](https://doi.org/10.1175/1520-0485(1982)012j0171:DWTSMI;2.0.CO;2)
- Osborn, T. 1996. The role of turbulent diffusion for copepods with feeding currents. *J. Plankton Res.* **18**: 185–195. doi:[10.1093/plankt/18.2.185](https://doi.org/10.1093/plankt/18.2.185)
- Ott, S., and J. Mann. 2000. An experimental investigation of the relative diffusion of particle pairs in three dimensional turbulent flow. *J. Fluid Mech.* **422**: 207–223. doi:[10.1017/S0022112000001658](https://doi.org/10.1017/S0022112000001658)
- Pécseli, H. L. 2016. Low frequency waves and turbulence in magnetized laboratory plasmas and in the ionosphere. IOP Publishing.
- Pécseli, H. L., and J. K. Trulsen. 2007. Turbulent particle fluxes to perfectly absorbing surfaces: A numerical study. *J. Turbul.* **8**: N42. doi:[10.1080/14685240701615986](https://doi.org/10.1080/14685240701615986)
- Pécseli, H. L., and J. K. Trulsen. 2010. Transit times in turbulent flows. *Phys. Rev. E* **81**: 046310. doi:[10.1103/PhysRevE.81.046310](https://doi.org/10.1103/PhysRevE.81.046310)
- Pécseli, H. L., J. K. Trulsen, and Ø. Fiksen. 2010. Predator-prey encounter rates in turbulent water: Analytical models and numerical tests. *Prog. Oceanogr.* **85**: 171–179. doi:[10.1016/j.pocean.2010.01.002](https://doi.org/10.1016/j.pocean.2010.01.002)
- Pécseli, H. L., J. K. Trulsen, and Ø. Fiksen. 2012. Predator-prey encounter and capture rates for plankton in turbulent environments. *Prog. Oceanogr.* **101**: 14–32. doi:[10.1016/j.pocean.2011.12.001](https://doi.org/10.1016/j.pocean.2011.12.001)
- Pécseli, H. L., J. K. Trulsen, and Ø. Fiksen. 2014. Predator-prey encounter and capture rates in turbulent environments. *Limnol. Oceanogr. Fluids Environ.* **4**: 85–105. doi:[10.1215/21573689-2768717](https://doi.org/10.1215/21573689-2768717)
- Pécseli, H. L., and J. K. Trulsen. 2016. Plankton's perception of signals in a turbulent environment. *Adv. Phys. X* **1**: 20–34. doi:[10.1080/23746149.2015.1136567](https://doi.org/10.1080/23746149.2015.1136567)
- Rothschild, B. J., and T. R. Osborn. 1988. Small-scale turbulence and plankton contact rates. *J. Plankton Res.* **10**: 465–474. doi:[10.1093/plankt/10.3.465](https://doi.org/10.1093/plankt/10.3.465)
- Saiz, E., and M. Alcaraz. 1991. Effects of small-scale turbulence on development time and growth of *Acartia grani* (Copepoda: Calanoida). *J. Plankton Res.* **13**: 873–883. doi:[10.1093/plankt/13.4.873](https://doi.org/10.1093/plankt/13.4.873)

- Saiz, E., and M. Alcaraz. 1992a. Enhanced excretion rates induced by small-scale turbulence in *Acartia* (Copepoda: Calanoida). *J. Plankton Res.* **14**: 681–689. doi:[10.1093/plankt/14.5.681](https://doi.org/10.1093/plankt/14.5.681).
- Saiz, E., and M. Alcaraz. 1992b. Free-swimming behaviour of *Acartia clausi* (Copepoda: Calanoida) under turbulent water movement. *Mar. Ecol. Prog. Ser.* **80**: 229–236. doi:[10.3354/meps080229](https://doi.org/10.3354/meps080229).
- Saiz, E., and T. Kiørboe. 1995. Predatory and suspension-feeding of the copepod *Acartia tonsa* in turbulent environments. *Mar. Ecol. Prog. Ser.* **122**: 147–158. doi:[10.3354/meps122147](https://doi.org/10.3354/meps122147).
- Saiz, E., A. Calbet, and E. Broglio. 2003. Effects of small-scale turbulence on copepods: The case of *Oithona davisae*. *Limnol. Oceanogr.* **48**: 1304–1311. doi:[10.4319/lo.2003.48.3.1304](https://doi.org/10.4319/lo.2003.48.3.1304).
- Sharqawy, M. H., J. H. Lienhard, and S. M. Zubair. 2010. Thermophysical properties of seawater: A review of existing correlations and data. *Desalination Water Treat.* **16**: 354–380. doi:[10.5004/dwt.2010.1079](https://doi.org/10.5004/dwt.2010.1079).
- Sharqawy, M. H., J. H. Lienhard, and S. M. Zubair. 2012. Erratum to thermophysical properties of seawater: A review of existing correlations and data [Desalination and Water Treatment, Vol. 16 (2010) 354–380]. *Desalination Water Treat.* **44**: 361–361. doi:[10.1080/19443994.2012.691709](https://doi.org/10.1080/19443994.2012.691709).
- Shkarofsky, I. P. 1969. Analytic forms for decaying turbulence functions, p. 289–295. *In* J. Fox (Ed.) *Turbulence in fluids and plasmas*. Polytechnic Press, New York.
- Stiansen, J. E., and S. Sundby. 2001. Improved methods for generating and estimating turbulence in tanks suitable for fish larvae experiments. *Sci. Mar.* **65**: 151–167. doi:[10.3989/scimar.2001.65n2151](https://doi.org/10.3989/scimar.2001.65n2151).
- Sundby, S., and P. Fossum. 1990. Feeding conditions of Arcto-Norwegian cod larvae compared with the Rothschild-Osborn theory on small-scale turbulence and plankton contact rates. *J. Plankton Res.* **12**: 1153–1162. doi:[10.1093/plankt/12.6.1153](https://doi.org/10.1093/plankt/12.6.1153).
- Sundby, S., B. Ellertsen, and P. Fossum. 1994. Encounter rates between first-feeding cod larvae and their prey during moderate to strong turbulent mixing. *ICES Mar. Sci. Symp.* **198**: 393–405.
- Tennekes, H. 1975. Eulerian and Lagrangian time microscales in isotropic turbulence. *J. Fluid Mech.* **67**: 561–567. doi:[10.1017/S0022112075000468](https://doi.org/10.1017/S0022112075000468).
- Tennekes, H., and J. L. Lumley. 1972. *A first course in turbulence*. The MIT press.
- Tilseth, S., and B. Ellertsen. 1984. Food consumption rate and gut evacuation processes of first-feeding cod larvae (*Gadus morhua* L.), p. 167–182. *In* E. Dahl, D. Danielssen, E. Moksness, and P. Solemdal [eds.], *The propagation of cod Gadus morhua* L. Flødevigen reportseries, v. 1, Institute of Marine Research, Norway.
- Trujillo, J. J., D. Trabucchi, O. Bischoff, M. Hofsäß, J. Mann, T. Mikkelsen, A. Rettenmeier, D. Schlipf, and M. Kühn. 2010. Testing of frozen turbulence hypothesis for wind turbine applications with a Staring Lidar. *Geophys. Res. Abstr.* **12**: EGU2010-5410.
- Wandel, C. F., and O. Kofoed-Hansen. 1962. On the Eulerian-Lagrangian transformation in the statistical theory of turbulence. *J. Geophys. Res.* **67**: 3089–3093. doi:[10.1029/JZ067i008p03089](https://doi.org/10.1029/JZ067i008p03089).

Acknowledgments

We thank Jan Even Øie Nilsen for help with the turbulence measurements, Bjørnar Ellertsen for assistance with the nauplii measurements, and Karen Gjertsen for providing Fig. 1. Valuable discussions with Øyvind Fiksen are gratefully acknowledged. Parts of the study were carried out under the project “Feeding conditions of cod larvae in an area with high tidal energy” funded with support from the Norwegian Research Council (NRC).

Conflict of Interest

None declared.

Submitted 27 June 2018

Revised 18 September 2018; 25 October 2018

Accepted 02 November 2018

Associate editor: Josef Ackerman